Hindawi
Advances in Civil Engineering
Volume 2022, Article ID 9460701, 12 pages
https://doi.org/10.1155/2022/9460701

Research Article

Experimental Investigation on the Vertical Bearing Characteristics of Jacked Piles in Saturated Silt Foundations under Excavation

Yong-Zhi Jiu,[1,2] **Zhen Zhang**,[1] **and Xiang-Yu Zhang**[1]

[1]*School of Civil Engineering and Architecture, Zhongyuan University of Technology, Zhengzhou 450007, China*
[2]*Key Laboratory of Geotechnical and Underground Engineering of Ministry of Education, Tongji University, Shanghai 200092, China*

Correspondence should be addressed to Yong-Zhi Jiu; jyz0912@163.com

Received 12 November 2021; Accepted 17 December 2021; Published 10 January 2022

Academic Editor: Zhiguo Zhang

A model test system for vertical bearing characteristics of the jacked piles in saturated soil foundations under excavation has been introduced. The system device comprises a soil pressure loading system, a model pile loading system, a soil vacuum saturation system, a model box, a model pile, and a control and data acquisition system. The soil vacuum saturation system designed for the model box of this test device can ensure that the saturated soil in the model box can reach a higher degree of saturation. Loading and unloading were conducted on the soil sample in the model box through the soil pressure loading system to simulate the soil excavation so that the soil sample and that in the field have the same stress state and history. The soil consolidation pressure, pile jacking pressure, pile tip force, soil consolidation settlement, and pile displacement at the top were collected and monitored in real time through the control and data acquisition system. This device is used to conduct an experimental study on the bearing characteristics of the jacked piles in saturated silt foundations under excavation. The results indicate that the static load test increases the residual pressure on the tip of the jacked pile while also increasing soil stiffness at pile tip and ultimate tip resistance, thereby increasing the pile top stiffness and ultimate load-carrying capacity. However, when the jacked pile is left undisturbed for the same time, the static load test on the jacked pile does not affect the pile skin friction resistance. There is a better linear relationship between the pile skin friction resistance and the undrained shear strength of the soil under the corresponding stress path during the static load test of the normally consolidated soil and the jacked pile after overburden pressure unloading. There is a good linear relationship between the ultimate resistance and the undrained shear strength of the soil under the corresponding stress path in pile sinking, normally consolidated soil, and during the static load test on jacked pile after unloading.

1. Introduction

In the construction of underground engineering structures or substructures of high-rise buildings, pile foundation is often set first. Then, the foundation pit (soil around the pile) is excavated, and the elevation is designed. The construction is carried out upward successively (the engineering piles are gradually loaded with the construction of buildings). The excavation unloading of soil around the pile will have a greater influence on the foundation pile at the pit bottom [1–4]. Troughton [5] and Wright and Doe [6] considered the tensile stress caused by excavation in the design of pile foundation. In order to avoid the fracture of the pile due to tension, it is advised to reinforce the whole length of the pile.

Many researchers have carried out experimental studies on the bearing characteristics of pile foundations under excavation. Mochtar and Edil [7] developed the test device and conducted laboratory model tests on the uplift pile in saturated clay. The results showed that the pile skin friction resistance was only related to the normal stress at the pile-soil interface. However, different from the pile foundation in field applications, the soil around the pile in the tests carried out by Mochtar and Edil [7] could be subjected to lateral deformation. Poulos and Chan [8] performed laboratory model tests on the pile foundation in

calcareous sand and found that when the lateral deformation of soil was constrained, the vertical overconsolidation ratio of soil around the pile would influence the pile skin friction. Chen et al. [9] simulated the soil excavation around piles by heaped loading and unloading of soil and conducted a model test study on the vertical compressive bearing characteristics of a single pile. Luo et al. [10] carried out a model test study on the influence of foundation pit excavation on bearing characteristics of uplift piles by excavating soil around piles with varying diameters and depths. Jia et al. [11, 12] conducted an experimental study on the stability of reinforced concrete piles and steel pipe piles under the excavation of soil around piles. In the above model tests, heaped loading, unloading, or excavation of the upper soil around piles, which were small and much different from the actual stress state of soil in the field, were carried out to simulate excavation.

The characteristics of the prototype of the conventional small-scale model cannot recur because the stress generated by its dead load is much lower than that of its prototype. Thus, the prototype shows pronounced nonlinearity [13]. One of the approaches to address this issue is to carry out centrifuge model testing, which many researchers did. Li et al. [14] and Hu et al. [15] carried out the centrifugal model tests on the bearing characteristics of uplift piles under excavation. Diao et al. [16] and Zheng et al. [17] carried out centrifuge model tests on compressive piles under excavation and showed that the vertical bearing capacity and stiffness of piles were significantly reduced by deep excavation. However, the centrifugal model test is relatively complex and costly, so it is not advisable for mass and systematic experimental studies on a particular problem.

Liu et al. [18] performed field measurements on the internal force and displacement of the pile at the pit bottom under construction in the process of foundation pit excavation. Yang et al. [19] studied the influence of the lateral movement of mucky soil on the existing jacked pile foundation during excavation unloading through a field test. The field test is more complicated and has minor reproducibility due to many parameters. Besides, the research focus in the tests mentioned above mainly involved nondisplacement piles. Currently, the experimental studies on the vertical bearing characteristics of jacked piles under the excavation unloading of soils are sparse. Therefore, developing a set of new test equipment has essential theoretical and practical value for the systematic experimental studies on the vertical bearing characteristics of the jacked piles under excavation unloading.

In this paper, a model test system for vertical bearing characteristics of the jacked piles under excavation is developed. This device is used to carry out experimental studies on pile sinking and bearing characteristics of the jacked piles in the saturated silt foundation under excavation, revealing the variation models on the residual stress and bearing characteristics of the jacked piles in saturated silt foundation before and after excavation.

2. Description of the Test System

The model test system for studying the vertical bearing characteristics of jacked piles under excavation includes a vertical soil pressure loading system, model pile loading system, soil vacuum saturation system, model box, model pile, and control and data acquisition system. Figures 1 and 2 show the schematic diagram, structural design drawing, and physical drawing for the model device.

The system is currently under review for the grant of the patent invention. Its basic working principle is as follows. The first deceleration stepping motor drives the turbine screw elevator, which further drives the spiral screw to rise and fall, transmitting the pressure to the reaction rod, and finally driving the pressure transmitting piston to apply the vertical load to the soil inside the model box. After the soil inside the model box is consolidated, the second deceleration stepping motor drives the spiral screw to rise and fall and applies the vertical load to the model pile, thus realizing the pile sinking and vertical loading test on the model pile. The soil consolidation pressure, pile top force, pile tip force, soil consolidation settlement, and pile top displacement in the whole test process are collected and monitored in real time through the control and data acquisition system.

2.1. Soil Pressure Loading System. The soil pressure loading system mechanism includes the upper crossbeam, the lower crossbeam, the first turbine screw elevator acting on the lower crossbeam, and the first deceleration stepping motor and force sensor monitored by the computer system as shown in Figure 1.

The overburden pressure loading and unloading of soil are set to simulate the excavation unloading of soil around piles. The soil pressure loading system has a measuring range of 0 to 300 kPa, a resolution ratio of 0.1 kPa, and an accuracy of 0.3% FS.

2.2. Model Pile Loading System. The model pile loading system includes an upper-pressure plate set up through four upright columns on the base pressure plate. A second turbine screw elevator is disposed in the center of the upper-pressure plate and connected to the second deceleration stepping motor. The second turbine screw elevator is downwardly connected to the pile top load sensor. The pile top force sensor is downwardly connected to the model pile, as shown in Figure 1. The model pile is vertically inserted into the soil sample through the round holes reserved for the upper crossbeam and the pressure transfer piston. The pile sinking test and vertical loading test are carried out on the model pile using the second deceleration stepping motor to drive the turbine screw to rise and fall and apply vertical load to the model pile. The model pile loading system has a measuring range of 0 to 3 kN, a resolution of 1 N, and an accuracy of 0.3% FS.

2.3. Structure of Model Box. The model box is made of transparent tempered glass material with an inner diameter of 40 cm and a height of 48 cm. A fixing ring is fixed on the pressure base plate by eight box positioning rods on the top of the model box. Sealing rings are arranged between the pressure base plate, the fixing ring, and the tempered glass to

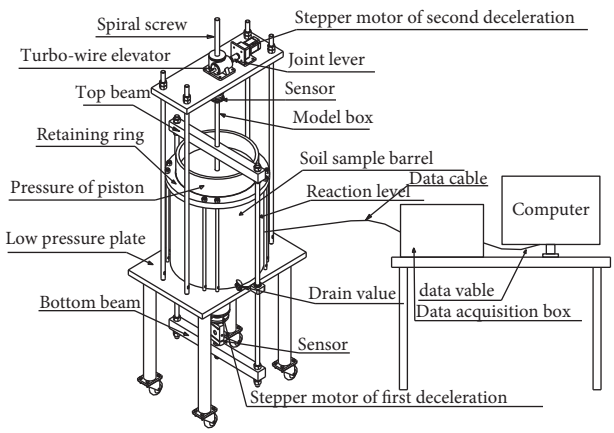

Figure 1: Schematic diagram for the model device.

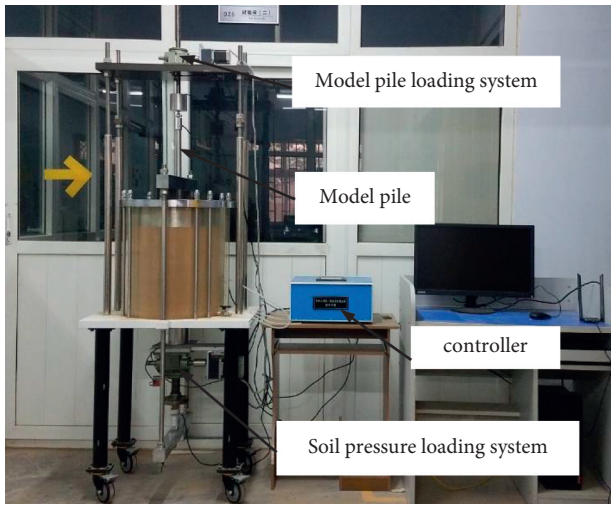

Figure 2: Physical drawing for the model device.

ensure the sealing performance of the model box. A water outlet is disposed of at the bottom of the model box, with a two-way ball valve switch installed for double-sided drainage during the consolidation of soil samples.

2.4. Model Pile. The model pile has a diameter of 2.5 cm, composed of pile tip, force sensor, and steel pipe with a length of 40 cm, as shown in Figure 3. The material is 304 stainless steel having an elastic modulus of 200 GPa. The pile tip force sensor has a measuring range of 0 to 3 kN, a resolution of 1 N, and an accuracy of 0.3% FS.

2.5. Soil Vacuum Saturation System. During the test on saturated soil, to ensure the soil has a high saturation, a soil vacuum saturation system is designed for the model box of the test device. A certain amount of prepared mud with a moisture content of 100% is added during the test at different times. Then, a sealing cover used for vacuuming is put on the top of the model box and connected to a vacuum pump for vacuuming saturation.

2.6. Control and Data Acquisition System. The control and data acquisition system is composed of a controller and supporting control software for the test system. The data acquisition system mainly focuses on soil consolidation pressure, pile top force, pile tip force, soil consolidation settlement displacement, and pile displacement at the top. Soil consolidation pressure, pile top force, and pile tip force are measured, fed back, and recorded in real-time by the force sensor. The soil consolidation settlement displacement and the vertical displacement of pile top are output by the corresponding deceleration stepping motor, which are calculated and recorded automatically by the software. The software interface can display the curves for variation of soil consolidation settlement displacement with time and that for pile top force and pile tip force with vertical displacement of pile top. The model pile can be loaded at a uniform speed and constant force through the control system.

2.7. Characteristics of the Test System. The innovative characteristics of the test device system are as follows:

(1) The maximum consolidation pressure of the soil in the model box can reach 300 kPa. The soil pressure loading system is used to perform loading and unloading of soil in the model box, making the soil in the model box and that in the actual engineering scenario to experience the same stress state and history.

(2) The soil vacuum saturation system can ensure that the soil used in the test reaches a high saturation degree and make the test show a higher reproducibility.

(3) The test device can realize uniform speed and constant-force loading of the model pile. The pile sinking test and vertical bearing characteristic test can be carried out on the jacked pile under different working conditions by applying different stress paths to the soil in the model box.

(4) The test system is controlled by software and operated automatically, which has higher accuracy and can perform data feedback and data storage in real-time.

3. Preliminary Application

3.1. Test Scheme. The model test system in this study is used to perform pile sinking and vertical bearing characteristic tests of the jacked pile in saturated silt foundation under excavation unloading. Table 1 shows the test parameters and details.

3.2. Test Procedure

3.2.1. Soil Sample Preparation. The soil used in the test was the silt from Zhengzhou. Figure 4 shows the particle size distribution (gradation curve) of the soil, while Table 2 enlists the fundamental physical properties of the soil.

After the test soil was dried, it was smashed with a rubber hammer and sifted through a sifter with a pore diameter of

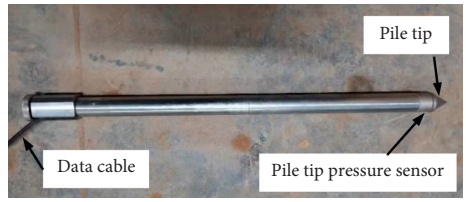

Figure 3: Physical diagram for a model pile.

Table 1: Model test scheme.

Number	Soil consolidation pressure (kPa)	Pile sinking of the jacked pile	Static load test	Vertical unloading pressure (kPa)	Static load test
1	50	Perform pile sinking test on the model pile after completing the consolidation	Perform static load test of a single pile two days after completing pile sinking	50 kPa	—
2	100				Perform static load test of the single pile after unloading rebound is stabilized
3	150				
4	100		—		

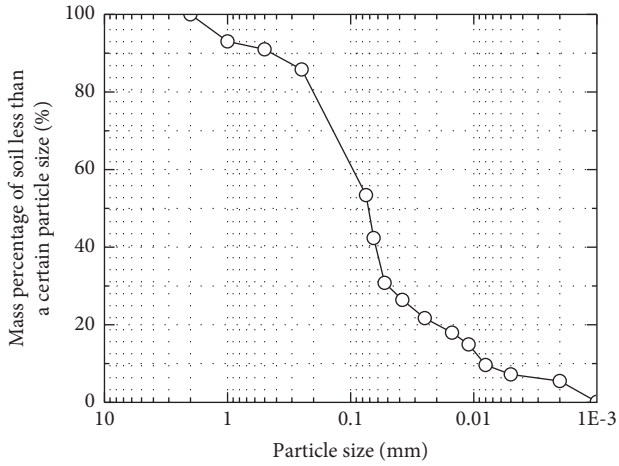

Figure 4: Soil particle gradation curve.

Table 2: Physical parameters for soil.

Plastic limit %	Liquid limit %	K_0	λ	κ	M
17	25.5	0.7	0.08	0.007	1.32

2 mm. The sifted soil was then mixed evenly. The slurry with a moisture content of 100% was prepared and thoroughly stirred. The mixed slurry was left undisturbed for 24 hours.

3.2.2. Soil Sampling and Saturation

(1) First, a layer of fine sand of 3 cm at the bottom of the model box was placed, and the drainage valve at the lower part of the model box was closed. Pure water was added to the model box to make the water surface 1 cm to 2 cm higher than the sand. The top of the model box was covered with a sealing cover and connected to the vacuum pump for vacuum saturation. After the vacuum degree in the model box reached more than −95 kPa, vacuuming was continued for 2 hours.

(2) A filter paper was put on the sand surface at the bottom of the model box, and the mixed silt slurry was poured into the model box at different times, with a height of the poured slurry being 7 cm to 8 cm each time. Vacuum saturation (continue vacuuming for 2 hours after the vacuum in the model box reached −95 kPa) was conducted, as shown in Figure 5. After the model box was filled with silt slurry and the last vacuuming was completed, the vacuum pump and the air exhaust valve were closed. The model box was subsequently kept in the vacuum state of above −95 kPa for 24 hours.

(3) After the silt slurry was filled and vacuum saturation was completed, the filter paper was placed on the top surface of the silt slurry in the model box, and 1 cm to 2 cm of fine sand was laid on the filter paper. After the fine sand remained still for several hours, the pressure transmitting piston was covered, and the upper and lower crossbeams were installed.

3.2.3. Soil Consolidation, Pile Sinking, and Vertical Loading Tests on the Jacked Pile

(1) The drainage valve at the bottom of the model box, the controller, and the computer were turned on. The consolidation pressure was applied to the soil in different stages in the model gradation by setting the control software. Through the software control interface, the curve for the variation of soil consolidation settlement with time was monitored in real time to determine whether the primary consolidation of soil in the model box was completed.

(2) After the primary consolidation of soil in the model box was completed, pile sinking was performed through the model pile loading system. The model pile was put vertically into the circular holes reserved

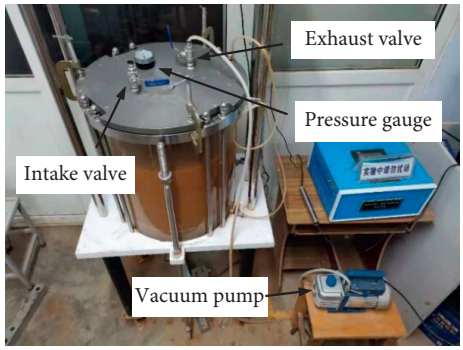

Figure 5: Vacuum saturation.

for the upper crossbeam and the pressure transmitting piston. The pile sinking rate (2 mm/s) and pile sinking displacement (190 mm) were set through the control software. After the pile sinking displacement reached a certain target value, the pile sinking ended. The variation of the residual pressure at the pile tip with time was monitored in real time through the software control interface.

(3) The model pile was left at a standstill for two days after pile sinking was completed. Meanwhile, the change of residual pressure at the pile tip was monitored to ensure the residual pressure at the pile tip was stable. The model pile loading system was used to conduct staged loading tests on the model pile.

(4) After the first static loading test was performed on the model pile and the model pile was left undisturbed for two days, the overburden pressure of the soil sample was unloaded to the target value through the software control system. The change of the residual pressure on the pile tip was monitored to ensure that the residual pressure on the pile tip was stabilized before the overburden pressure of the soil was unloaded. After the unloading of the overburden pressure, the soil rebounds. Therefore, the next test was conducted when it was confirmed that the soil rebound was stable based on monitoring through the software control interface.

(5) Static loading test was carried out on the model pile after the soil unloading, and the subsequent rebound was stabilized. After the test was over, the overburden pressure of soil was unloaded, and the model pile was pulled out. The test equipment was dismantled, and the soil samples in the model box were cleared away, thus completing the test.

4. Analysis of Model Test Results

4.1. Soil Consolidation and Pile Sinking Test of Jacked Pile. The consolidation loading of soil in the model box was performed through step loading, and the pressure levels were 2 kPa, 12.5 kPa, 25 kPa, 50 kPa, 100 kPa, and 150 kPa, respectively. Through the software control interface, the curve for the variation of soil consolidation settlement with time was monitored in real time to determine whether the primary consolidation of soil in the model box was completed. After completing each consolidation stage, the next stage of the load was applied.

In order to verify the effects of the vacuum saturation system, consolidation and model pile sinking tests were carried out on soil undergoing the vacuum saturation and that not undergoing any vacuum saturation, respectively. The test results are shown in Figures 6 and 7. It can be seen that the consolidation settlement rate of vacuum-saturated soil is significantly higher than that of soil without being vacuum-saturated (Figure 6). Also, when pile sinking occurs in the vacuum-saturated soil, pile tip resistance increases gradually with pile displacement and eventually tends to be stable (Figure 7). However, the curve for pile sinking in the soil not undergoing vacuum saturation indicates that when the pile displacement is smaller, the pile tip resistance increases with the increase of the pile tip displacement. As soon as the pile tip resistance begins to decline after reaching the peak value, the pile tip resistance is smaller than that in the vacuum-saturated soil. When the soil in the model box was excavated after the test was finished, it was found that on the surface layer of soil without being vacuum-saturated, there was a 2 cm hard thick crust. It was evident that the soil below the hard crust had become softer. During vacuum saturation of silt slurry, it was found that when the pressure in the model box reached more than −95 kPa, lots of bubbles poured out from the silt slurry, as shown in Figure 8. Therefore, there were more tiny bubbles in the silt slurry without being vacuum-saturated. The bubbles moved up gradually during the loading and consolidation process, resulting in a higher unsaturation degree of surface soil in the model box. Due to the poor permeability of the unsaturated soil, the hard crust on the surface of the soil sample was formed, influencing the consolidation of the lower soil.

Figure 9 shows the curves for the variation consolidation settlement displacement of soil in the model box with time, under the last consolidation pressure when the maximum vertical consolidation pressure was 50 kPa, 100 kPa, and 150 kPa, respectively. It can be seen that under different consolidation pressures, the primary consolidation of the soil in the model box is completed, and the completion time for primary consolidation is the same.

After the consolidation of saturated silt foundation was completed, the pile sinking tests of the jacked pile with overburden pressure of 50 kPa, 100 kPa, and 150 kPa were carried out. Figures 10 and 11 show the relation curves for pile sinking resistance-pile sinking displacement and pile skin friction-pile sinking displacement, respectively.

It is seen that when pile sinking displacement is smaller, the pile sinking resistance increases with the increase of pile sinking displacement (Figure 10). With the increasing pile sinking displacement, the increase of pile sinking resistance gradually slows down and tends to increase linearly when reaching a certain depth. Pile tip resistance changes with pile sinking displacement, showing the same change trend as that of pile sinking resistance in the early stage—the difference being that as the pile sinking displacement increases, after the pile sinks to a certain depth, the pile tip resistance

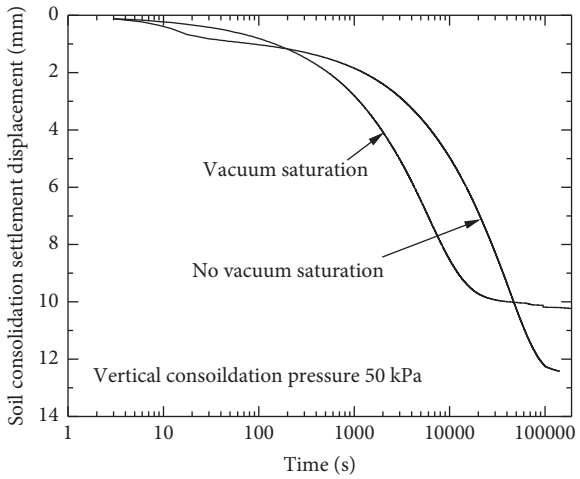

Figure 6: Displacement-time curves for soil consolidation settlement.

Figure 8: Bubbles generated from vacuum-saturated silt slurry.

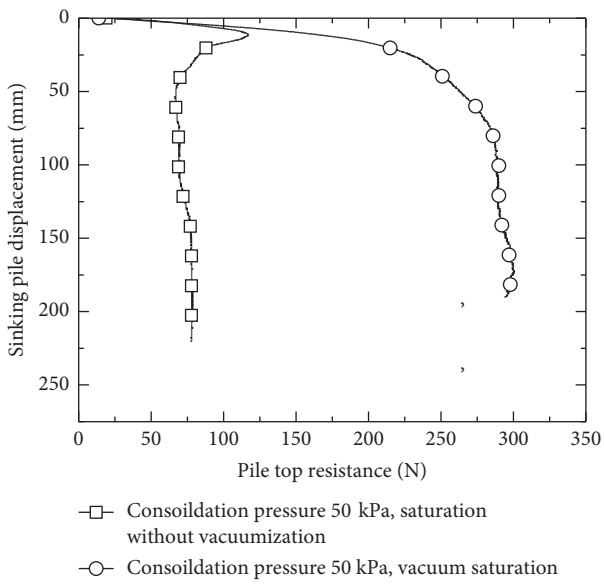

Figure 7: Relationship curve for pile tip resistance-pile sinking settlement.

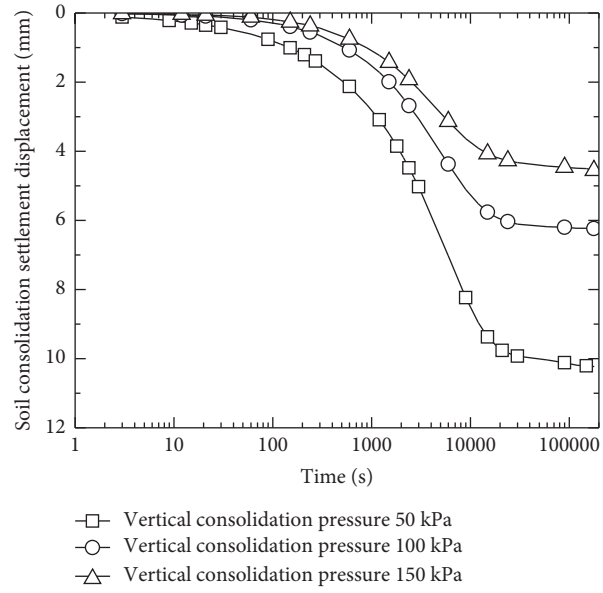

Figure 9: Displacement-time curves for soil consolidation settlement.

remains unchanged as the pile sinking displacement increases. This depth is called the critical depth. It can be seen from Figure 11 that the total ultimate friction resistance of the pile increases linearly with the increase of pile sinking displacement.

4.2. Analysis of the Residual Pressure on Pile Tip of the Jacked Pile. During pile sinking, the jacked pile disturbs the soil, causing the soil to suffer shear failure. This results in the generation of excess pore water pressure in the soil around the pile sides and lower part of pile tip and subsequent gradual decrease of the soil strength. After pile sinking is finished, the strength of soil around piles and that on the pile tip increase gradually with the dissipation of excess pore water pressure in the soil, which increases the soil strength, thus changing the residual pressure at the pile tip. Figure 12 shows the variation of residual pressure at pile tip with time at different stages after pile sinking of the jacked pile is finished.

After the sinking of the jacked pile is finished, the residual pressure at the pile tip gradually increases with time and eventually tends to be stable (Figure 12(a)). Also, the larger the overburden consolidation pressure of soil, the larger is the residual pressure at the pile tip after the pile sinking. By comparing Figure 12(b) and Figure 12(a), it can be inferred that after the static load test is completed, the residual pressure at the pile tip increases more rapidly. The final value of residual pressure at the pile tip after the static load test is significantly greater than that obtained after the pile sinking; i.e., the static load test increases the residual pressure at the pile tip.

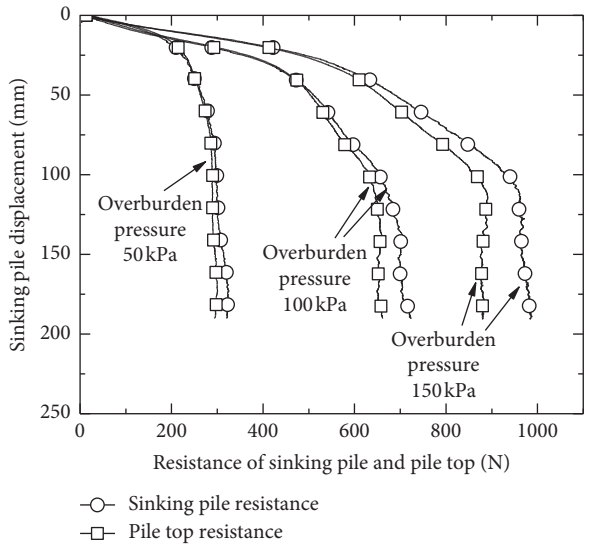

Figure 10: Relation curves for pile sinking (pile tip) resistance-pile sinking displacement.

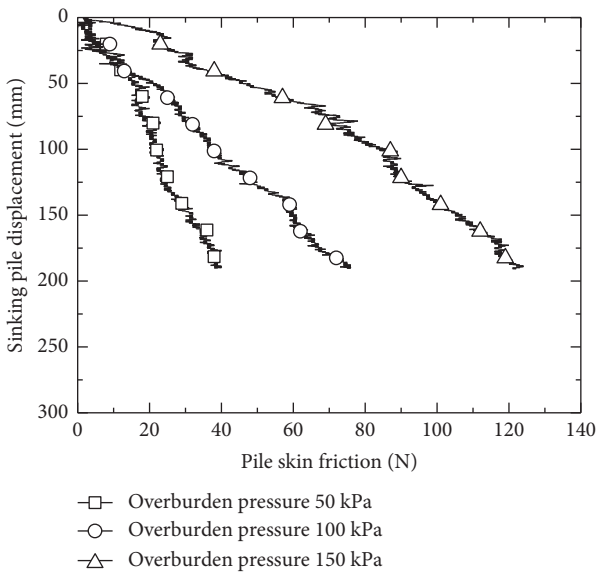

Figure 11: Relation curves for pile skin friction-pile sinking displacement.

After the jacked pile in normally consolidated soil is left to stand for two days after the static load test is completed (ensuring that residual pressure at the pile tip is stabilized), the unloading of the overburden pressure soil is performed. Soil unloading causes the soil to rebound, and the residual pressure at the pile tip drops suddenly (Figure 12(c)). The greater the overburden pressure unloading of soil, the greater the declining range of residual pressure at the pile tip.

4.3. Analysis on Bearing Characteristics of the Jacked Pile under Excavation Unloading. After unloading of soil around the jacked pile, the soil rebounds, as shown in Figure 13. The larger the unloading amount (of overburden pressure on soil), the larger is the corresponding rebound.

Figure 14 through Figure 15 show the results of static load tests on the jacked pile when the overburden pressure was 50 kPa, 100 kPa, and 150 kPa, respectively. When the overburden pressure of 100 kPa and 150 kPa (after static load test on the jacked pile was completed) was unloaded to 50 kPa, the soil rebound became stable.

It can also be seen that the greater the overburden pressure of normally consolidated soil, the greater the ultimate bearing capacity, pile top stiffness, ultimate tip resistance, and skin friction of the jacked pile. It is observed that under the same overburden pressure, the greater the overconsolidation ratio of soil, the greater the ultimate bearing capacity, pile top stiffness, ultimate tip resistance, and skin friction of the jacked pile. The ultimate bearing capacity of the pile top when soil pressure is 150 kPa is greater than that after unloading (the overburden pressure is unloaded from 150 kPa to 50 kPa), but the stiffness of the pile top after the unloading of overburden pressure has a minor change (Figure 14). The ultimate bearing capacity of the pile top at the soil pressure of 100 kPa changes less than that of the pile tip after unloading (the overburden pressure is unloaded from 100 kPa to 50 kPa). The stiffness of the pile top after unloading is slightly greater than that before unloading. When soil pressure is 150 kPa, the ultimate pile tip resistance is greater than that after unloading (overburden pressure is unloaded from 150 kPa to 50 kPa). However, after unloading of overburden pressure, the pile tip stiffness exhibits a minor change (Figure 16). The ultimate pile tip resistance at the soil pressure of 100 kPa changes less than the ultimate bearing capacity of pile tip after unloading (the overburden pressure is unloaded from 100 kPa to 50 kPa). However, an anomaly is that the pile tip stiffness after unloading is slightly greater than before unloading occurs.

Due to the residual pressure on the jacked pile, there is a negative friction resistance existing along the pile length (Figure 15). This negative friction resistance gradually decreases with the increasing pile top displacement and transforms into positive friction resistance. It then decreases slightly after reaching the ultimate friction resistance, where it remains stable (residual friction resistance). It can also be seen from Figure 15 that unloading of overburden pressure of soil around the pile causes a decline in the pile skin friction—the greater the unloading value, the greater the decreasing range of pile skin friction.

Figures 14 through 16 show that after the static load test on the jacked pile, the corresponding normally consolidated soil was left to remain there for a certain period; then, the overburden pressure unloading was done, and the static load test on the jacked pile was carried out under excavation unloading. An "abnormality" observed from the analysis of Figures 14 and 16 is that the stiffness of pile top and pile tip increases after unloading (comparing the static load test results of the model pile at the soil pressure of 100 kPa with that when overburden pressure is unloaded from 100 kPa to 50 kPa). It can be inferred that the static load test on the normally consolidated soil affects the follow-up static load

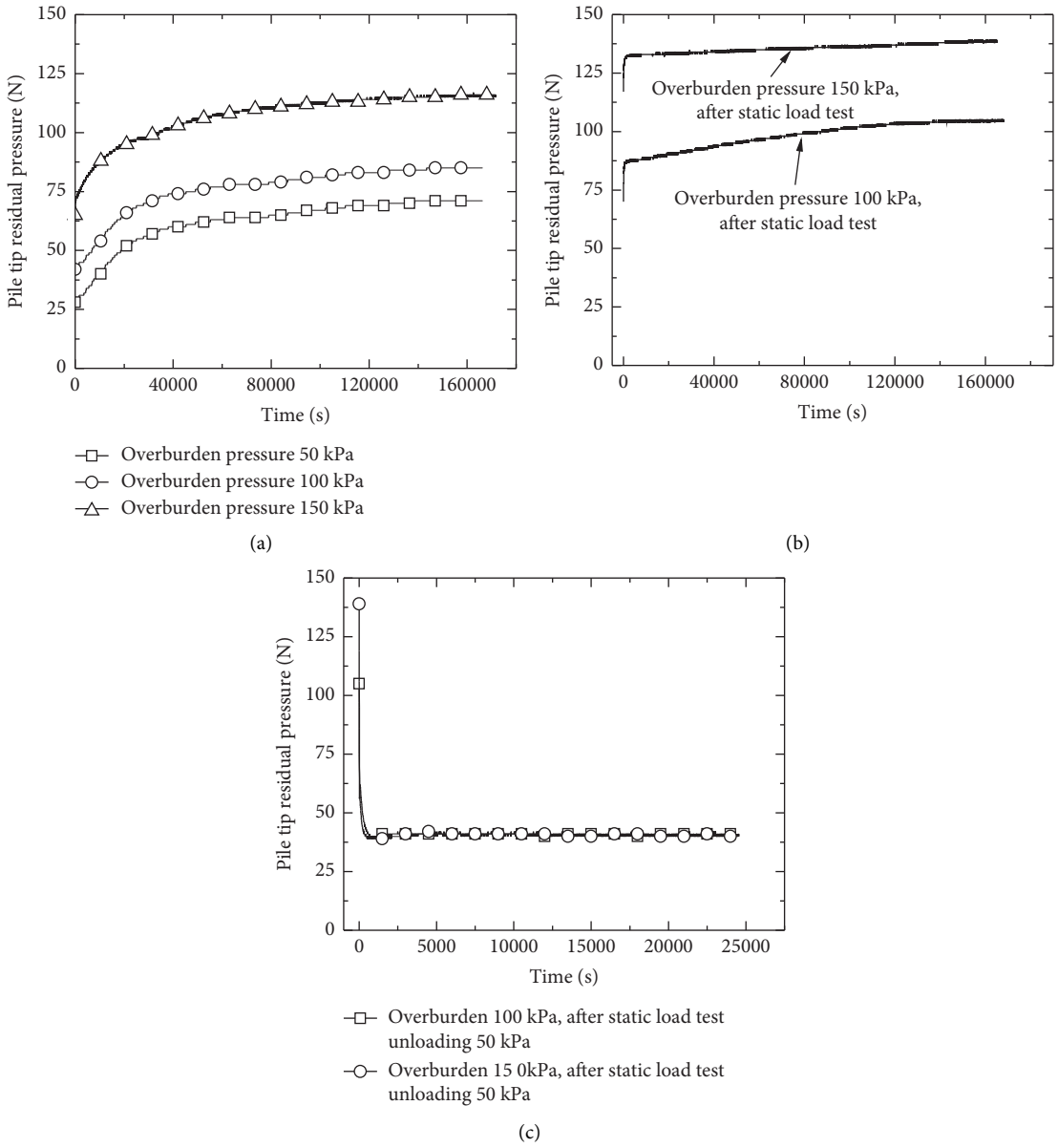

Figure 12: Variation of residual pressure at pile tip with time. (a) After completion of pile sinking. (b) After the static load test. (c) After unloading.

test results after unloading. In order to confirm this effect, the following tests were carried out in this study.

(i) With the overburden pressure of 100 kPa, the pile sinking test was carried out after the soil consolidation was completed and after letting it at a standstill for two days (no static load test on normally consolidated soil was carried out)

(ii) The overburden pressure was unloaded to 50 kPa, and the static load test under unloading was carried out after the soil rebound after unloading was stable

The test results are shown in Figure 17 through Figure 18.

As shown in Figures 17 and 19, no static load test was conducted when the overburden pressure was 100 kPa. The ultimate bearing capacity, pile top stiffness, ultimate tip resistance, and pile tip stiffness of the jacked pile obtained after the overburden pressure of soil (directly unloaded to 50 kPa) were all less than the values before unloading (the static load test result obtained when the overburden pressure of soil was 100 kPa). It is clear from Figure 18 that the pile skin friction after unloading of overburden pressure remains the same regardless of whether or not the load test was conducted on the jacked pile in normally consolidated soil before unloading of overburden pressure. Also, the change in pile skin friction with pile top displacement remains consistent; i.e., the static load test on the jacked pile before the unloading of overburden pressure has practically no effect on the pile skin friction during the static load test and after the unloading. Based on the above analysis, it can be concluded that the static load test on the pile can improve the soil stiffness and ultimate pile tip resistance, thereby increasing the ultimate bearing capacity and stiffness of the

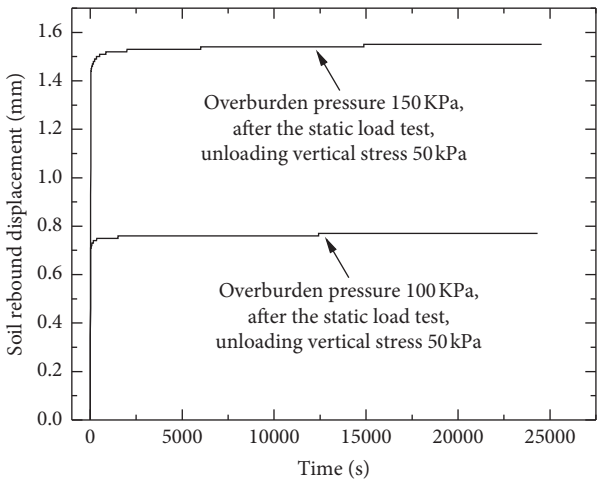

Figure 13: Soil rebound displacement versus time plots.

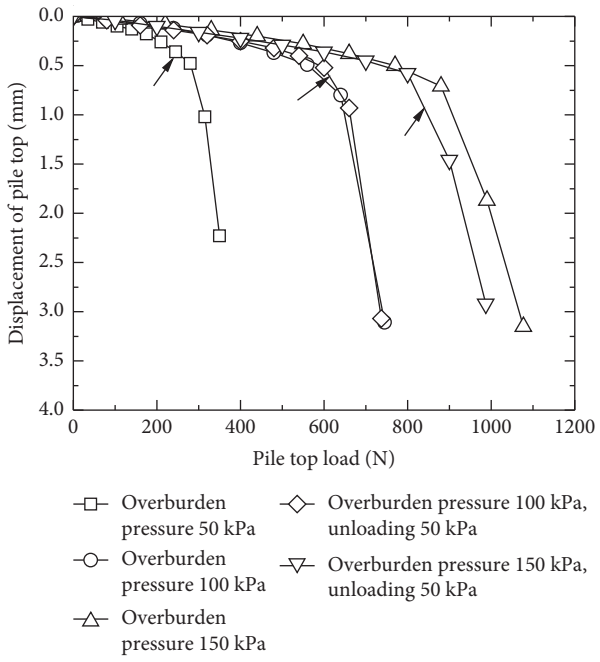

Figure 14: Load-displacement curves for the pile top.

pile top. However, when the jacked pile is left undisturbed for the same time, the static load test of the jacked pile does not affect the pile skin friction.

4.4. Comprehensive Analysis of Bearing Characteristics of the Jacked Pile in Saturated Silt Foundation. Tomlinson [20] believed that the ultimate pile side friction was related to the undrained shear strength of pile side soil and gave the following formula for calculating the ultimate pile side friction.

$$\tau_f = \alpha c_u, \tag{1}$$

where τ_f is the pile skin friction capacity, α is the pile side friction coefficient, and c_u is the undrained shear strength of soil around pile.

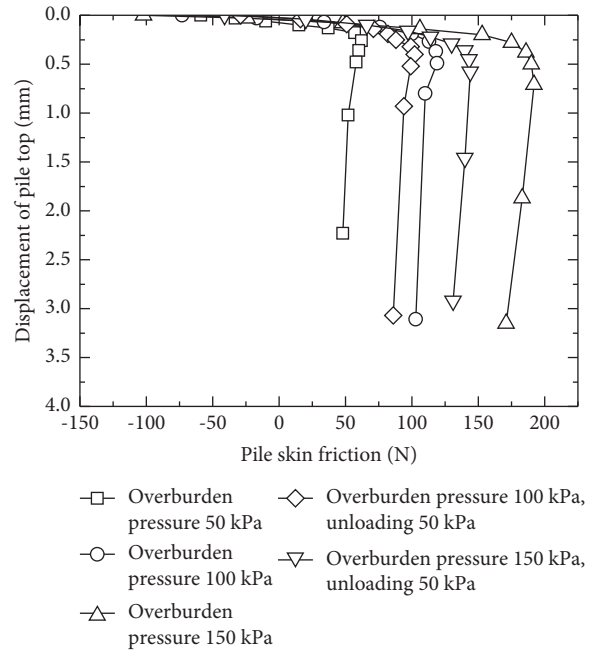

Figure 15: Pile skin friction versus displacement of pile top.

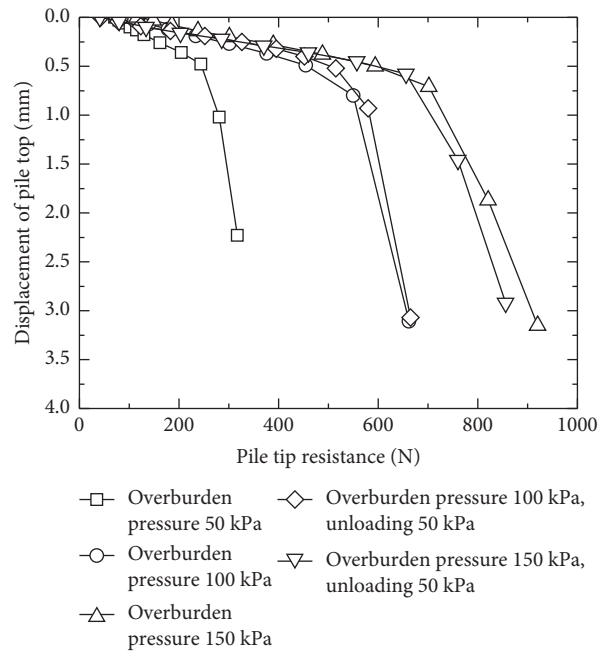

Figure 16: Pile tip resistance versus displacement of pile top.

Based on the analysis of a large number of data, Coduto [21] believed that the values of α and c_u were related and suggested that the α value of driven piles should be calculated by the following formula:

$$\alpha = \begin{cases} 1 & (c_u \le 32\text{kPa}) \\ 0.35 + 170 c_u^{-1.6} & (c_u > 32\text{kPa}) \end{cases} \tag{2}$$

Lacasse, Boisard [22], and API [23] have studied the value of α and given the calculation formula, as shown in

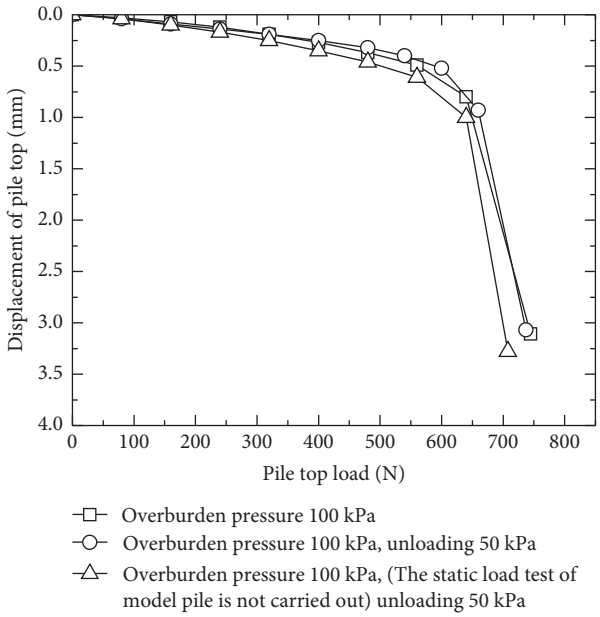

Figure 17: Pile top load versus pile top displacement.

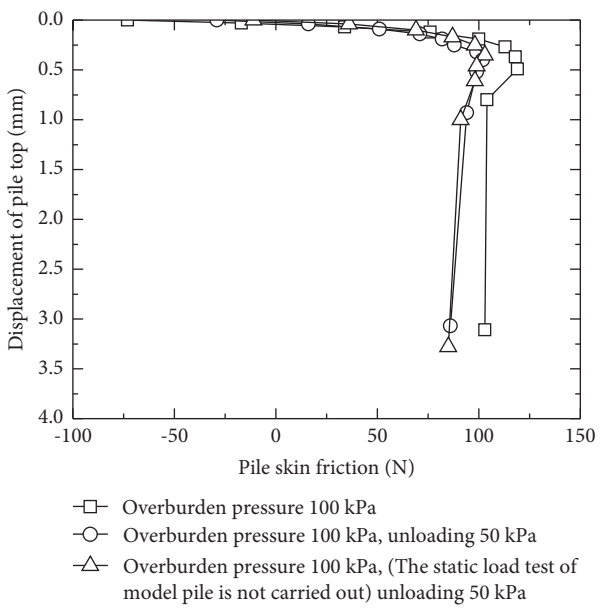

Figure 18: Pile skin friction versus pile top displacement.

$$\alpha = \begin{cases} 0.5\left(\dfrac{\sigma_{v0}'}{c_u}\right)(/)^{0.5} & \left(\dfrac{c_u}{\sigma_{v0}'} \le 1.0\right) \\ 0.5\left(\dfrac{\sigma_{v0}'}{c_u}\right)^{0.25} & \left(\dfrac{c_u}{\sigma_{v0}'} > 1.0\right) \end{cases}, \quad (3)$$

where σ_{v0}' is the vertical effective stress of the soil around the pile.

The GDS stress path triaxial tester was used in this study to systematically study the relationship between the strength characteristics of soil in saturated silt foundation and the

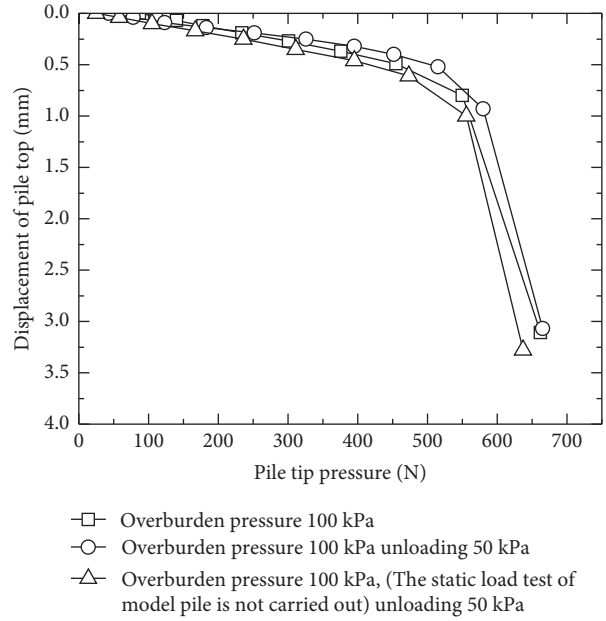

Figure 19: Pile tip pressure versus pile top displacement.

bearing characteristics of the jacked pile. A stress path triaxial test was conducted on the soil used in the model test. The undrained shear strength of saturated silt under the same stress path as the soil in the model box was obtained and compared with the pile skin friction and tip resistance during pile sinking, as well as the pile skin friction and the ultimate tip resistance in the static load test. The results are shown in Table 3 and Figure 20.

As is shown in Table 3 and Figure 20, when pile sinking is finished, a better linear relationship is shown between the pile skin friction τ_f and the undrained shear strength c_u of soil under the corresponding stress path; the formula $\tau_f = 0.21c_u$ in Figure 20 is obtained by data fitting. The pile skin friction τ_f in the process of static load test of the jacked pile in normally consolidated soil and after unloading of overburden pressure and the undrained shear strength c_u of soil under the corresponding stress path also show a better linear relationship; the formula $\tau_f = 0.14c_u$ in Figure 20 is obtained by data fitting. The pile skin friction capacity in the static load test is significantly greater than that during pile sinking; i.e., the pile skin friction resistance shows noticeable timeliness.

It can also be seen from Figure 20 that the pile side ultimate friction obtained from the calculation formula of α value recommended by Coduto (1994) [21] and API (1993) [23] (equations (2) and (3)) is significantly higher than the test results in this paper. The test result α in this paper is approximately constant and is not related to the vertical overconsolidation ratio of soil around the pile. Therefore, the overconsolidation ratio of the soil around the pile has no effect on the ultimate frictional resistance of the jacked pile in saturated silt soil.

It can also be seen from Tables 3 and 4 and Figure 21 that there is a linear relationship between the ultimate tip resistance $F_N/\pi r^2 c_u$ and the undrained shear strength c_u of soil

Table 3: Ratio of ultimate friction resistance to the undrained shear strength of the soil.

σ_v (kPa)	c_u.(kPa)	Static load testing		When pile sinking of the jacked pile is finished	
		τ_f (kPa)	(τ_f/c_u)	τ_f (kPa)	(τ_f/c_u)
50	20.2	4.8	0.238	3	0.149
100	43.8	9.2	0.210	5.8	0.132
150	65	14.6	0.225	9.4	0.145
100 ⟶ 50	40	7.8	0.195	—	—
150 ⟶ 50	54	11.1	0.206	—	—

Note. σ_v denotes overburden pressure of soil.

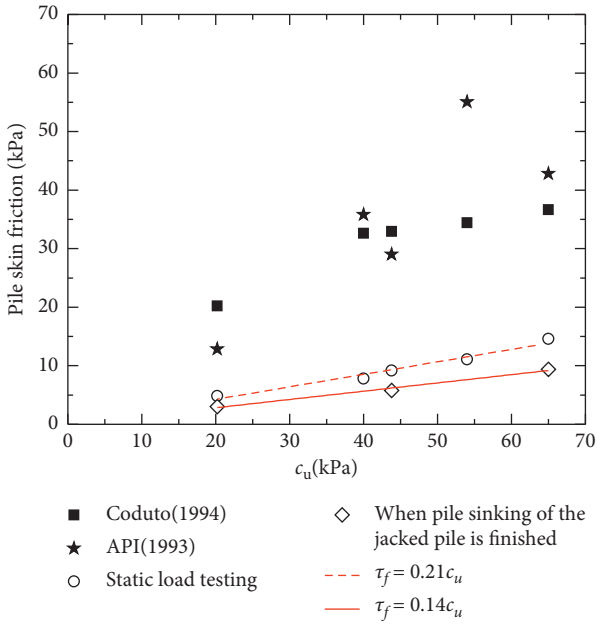

Figure 20: Pile skin friction versus undrained shear strength of the soil.

Table 4: Ratio of ultimate tip resistance to the undrained shear strength of the soil.

σ_v (kPa)	c_u (kPa)	Static load testing		When pile sinking of the jacked pile is finished	
		F_N (N)	$F_N/\pi r^2 c_u$	F_N (N)	$F_N/\pi r^2 c_u$
50	20.2	317	31.97	295	29.75
100	43.8	665	30.93	661	30.74
150	65	920	28.83	880	27.58
100 ⟶ 50	40	637	32.44	—	—
150 ⟶ 50	54	856	32.29	—	—

Note. R denotes the pile radius; F_N denotes ultimate tip resistance.

under the corresponding stress path in a pile sinking in normally consolidated soil. The formula $F_N/\pi r^2 = 30c_u$ in Figure 21 is obtained by data fitting.

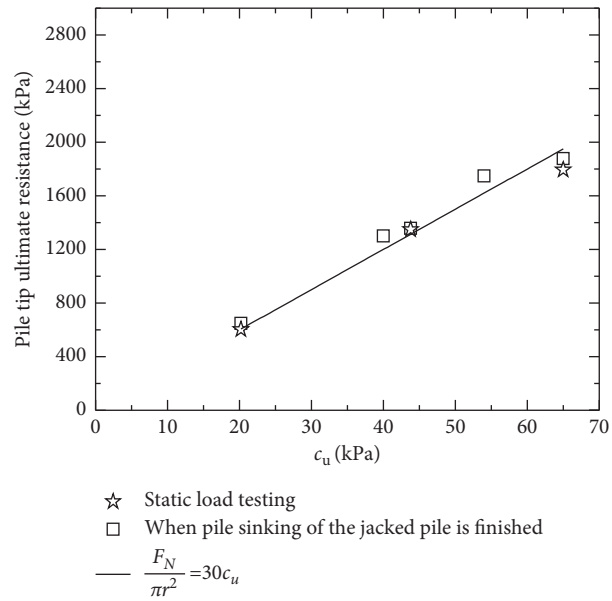

Figure 21: Ultimate pile tip resistance versus undrained shear strength of the soil.

5. Conclusion

In this paper, a model test system for vertical bearing characteristics of jacked piles under excavation is developed. Performing vacuum saturation on the slurry in the model box can ensure that the soil in the model box reaches a higher saturation. The overburden pressure and stress path of the soil can be precisely controlled by loading and unloading of soil in the model box through the soil pressure loading system so that the soil has the same stress state and history as that in practical engineering. The model test system developed in this paper is used to carry out pile sinking and bearing characteristics tests on jacked piles in saturated silt foundations under excavation. The main conclusions are concluded as follows.

(1) Under the same overburden pressure conditions, the greater the overconsolidation ratio of soil, the greater the ultimate bearing capacity, pile top stiffness, pile tip ultimate bearing capacity, and skin friction of jacked piles.

(2) Static load test increases the residual pressure at the pile tip, and the soil around the pile rebounds after unloading, resulting in the decrease in the residual pressure at the pile tip. The larger the overburden pressure unloading of soil, the greater the decreasing range for residual pressure of pile tip.

(3) Static load test on jacked pile can improve the soil stiffness and ultimate pile tip resistance and increase the ultimate bearing capacity of pile top and pile top stiffness. However, when the jacked pile is left undisturbed for the same time, the static load test of the jacked pile does not affect the pile skin friction.

(4) There is a linear relationship between the pile skin resistance τ_f and the undrained shear strength c_u of soil under the corresponding stress path during pile sinking of the jacked pile in the saturated silt foundation. There is also a linear relationship between the pile skin friction τ_f during the static load test of the jacked pile in normally consolidated soil and after unloading of overburden pressure and the undrained shear strength c_u of soil under the corresponding stress path. Besides, a linear relationship is shown between the ultimate tip resistance $F_N/\pi r^2$ and the undrained shear strength c_u of soil under the corresponding stress path in pile sinking and normally consolidated soil and during the static load test of the jacked pile after unloading.

Data Availability

The raw/processed data required to reproduce these findings cannot be shared at this time as the data also form part of an ongoing study.

Conflicts of Interest

The authors declare that they have no conflicts of interest.

Acknowledgments

This work was financially supported by the National Natural Science Foundation for Young Scientists of China (Grant no. 51608548) and the Young College Teacher Training Program Project of Henan Province (Grant no. 2018GGJS106).

References

[1] Y. Iwasaki, H. Watanabe, M. Fukuda, A. Hirata, and Y. Hori, "Construction control for underpinning piles and their behaviour," *Géotechnique*, vol. 44, no. 4, pp. 681–689, 1994.

[2] C. J. Lee, A. Altabbaa, and M. D. Bolton, "Development of tensile force in piles in swelling ground," in *Proceedings of the Third International Conference on Soft Soil*, pp. 345–350, Hong Kong, December 2001.

[3] G. Zheng, S. Y. Peng, C. W. W. Ng, and Y. Diao, "Excavation effects on pile behaviour and capacity," *Canadian Geotechnical Journal*, vol. 49, no. 12, pp. 1347–1356, 2012a.

[4] H. G. Zhu and J. P. Sun, "Effect of basal soil heave on piles during deep excavation in Shanghai," *Geotechnical Engineering World*, vol. 8, no. 3, pp. 43–46, 2004.

[5] V. M. Troughton, "The design and performance of foundations for the Canary Wharf development in London Docklands," *Géotechnique*, vol. 42, no. 3, pp. 381–393, 1992.

[6] RH. Wright and G. Doe, "Littile britain project: construction of basement," *Proceedings of International Conference on Piling and Deep Foundations*, vol. 1, pp. 221–230, 1989.

[7] I. B. Mochtar and T. B. Edil, "Shaft resistance of model pile in clay," *Journal of Geotechnical Engineering*, vol. 114, no. 11, pp. 1227–1244, 1988.

[8] H. G. Poulos and K. E. Chan, "Laboratory study of pile skin friction in calcareous sand," *Civil Engineering Research Report No.R486*, University of Sydney, Sydney, 1984.

[9] J. J. Chen, Q. Wu, J. H. Wang, and X. H. Wang, "Model tests on bearing capacity of single pile influenced by excavation," *Chinese Journal of Geotechnical Engineering*, vol. 32, no. S2, pp. 85–88, 2010.

[10] Y. W. Luo, Q. Hu, Y. M. Chen, and D. S. Ling, "Model tests on ultimate uplift capacity of piles under excavation," *Chinese Journal of Geotechnical Engineering*, vol. 33, no. 3, pp. 427–432, 2011.

[11] Q. Jia, C. L. Li, and X. Zhang, "Study of reinforced concrete pile buckling stability under excavation conditions," *Journal of Building Structures*, vol. 40, no. 11, pp. 247–254, 2019.

[12] Q. Jia, H. D. Wang, and X. Zhang, "Study on bucking stability of steel tube pile during surrounding soil excavation," *China Civil Engineering Journal*, vol. 51, no. 9, pp. 102–109, 2018.

[13] Z. Feng and Y. P. Yin, "Statw of the art review of geotechnical centrifuge modeling test in China," *Journal of Engineering Geology*, vol. 19, no. 3, pp. 323–331, 2011.

[14] J. J. Li, M. S. Huang, W. D. Wang, and Z. Chen, "Centrifugal model tests on bearing capacity of uplift piles under deep excavation," *Chinese Journal of Geotechnical Engineering*, vol. 32, no. 3, pp. 388–396, 2010.

[15] Q. Hu, D. S. Ling, L. G. Kong, Y. W. Luo, M. Niu, and Z. Chen, "Effects of deep excavation on uplift capacity of piles by centrifuge tests," *Chinese Journal of Geotechnical Engineering*, vol. 35, no. 6, pp. 1076–1083, 2013.

[16] Y. Diao, *Studies on Effects of Super-deep Excavation on the Bearing Capacity and Settlement Behavior of Compression Piles beneath the Basement*, Tianjin University, Tianjin, China, 2011.

[17] G. Zheng, L. M. Zhang, Q. Wang, and C. Q. Liu, "Field observation and finite element analysis of effect of overlying excavation on piles," *Journal of Tianjin University*, vol. 45, no. 12, pp. 1062–1070, 2012b.

[18] C. Liu, Y. Guo, G. Zheng, and C. D. Yan, "Research on effect of deep excavation on force deformation characteristic of piles in pit," *Journal of Building Structures*, vol. 42, no. 5, p. 177, 2021.

[19] S. C. Yang, M. Y. Zhang, J. P. Guan, and Z. L. Li, "Experimental study on the influence of excavation unloading on existing static pressure piles in silt soil," *Journal of Shandong Agricultural University (Natural Science Edition)*, vol. 52, no. 1, pp. 98–104, 2021.

[20] M. J. Tomlinson, "The adhesion of piles driven in clay soils,"vol. 2, pp. 66–71, in *Proceedings of the 4th International Conference on Soils Mechanics and Foundation Engineering*, vol. 2, pp. 66–71, Thomas Telford Ltd, London, UK, 1957.

[21] D. P. Coduto, *Foundation Design, Principles and Practices*, Prentice-Hall, Englewood Cliffs, N.Y, 1994.

[22] S. Lacasse and P. Boisard, "Consequence of the new API RP2A guideline for piles in soft clays," in *Proceedings of the 13th international Conference on Soil Mechanics and Foundation Engineering*, pp. 527–530, New Delhi, India, January 1994.

[23] American Petroleum Institute (Api), *Recommended Practice for Planning, Designing and Constructing Fixed Offshore Platforms*, American Petroleum Institute, Dallas, 20th edition, 1993.